Synthesis and Characterization of Some Benzidine-Based Azomethine Derivatives with Molecular Docking Studies and Anticancer Activities

Musa Erdoğan
Kafkas University: Kafkas Universitesi
ali yeşildağ (aliyesildag@yahoo.com)
Kafkas Universitesi Mühendislik ve Mimarl?k Fakültesi https://orcid.org/0000-0002-7217-0899
Barış Yıldız
Kafkas University: Kafkas Universitesi
Burak Tüzün
Cumhuriyet Üniversitesi: Sivas Cumhuriyet Universitesi
Özkan Özden
Kafkas University: Kafkas Universitesi

Research Article

Keywords: Azomethine derivatives, Anticancer activities, MDA-MB-231, DLD1, Molecular docking, ADME/T.

Posted Date: May 20th, 2021

DOI: https://doi.org/10.21203/rs.3.rs-528128/v1

Abstract

In this paper, a new benzidine-based azomethine derivate **2** with a proposed new mechanism and its two derivatives **4a-b** have been designed, synthesized and characterized by ^{1}H, ^{13}C NMR, FT-IR, and HRMS spectroscopic techniques, and their anticancer properties were investigated. The target compounds **2**, **4a-b** were obtained with excellent yields (91% and above) by condensation of benzidine (**1**) with three different aldehyde derivatives (formaldehyde, benzaldehyde **3a** or *p*-nitrobenzaldehyde **3b**) in refluxing EtOH. Surprisingly, treatment of benzidine (**1**) with formaldehyde afforded $N^4,N^4,N^{4'},N^{4'}$-tetrakis(ethoxymethyl)-[1,1'-biphenyl]-4,4'-diamine (**2**). The anticancer properties of these benzidine derivatives **2**, **4a-b** against two cell lines (MDA-MB-231 human breast adenocarcinoma and DLD1 human colorectal adenocarcinoma cell lines) were investigated with a colorimetric assay using the tetrazolium salt WST-8 (2-(2-methoxy-4-nitrophenyl)-3-(4-nitrophenyl)-5-(2,4-disulfophenyl)-2*H*-tetrazolium, monosodium salts). The obtained results showed that the benzidine-based azomethine derivatives **2**, **4a-b** had a significant effect against human breast cancer cell line (MDA-MB-231). Then, molecular docking calculations were made to compare the biological activities of benzidine-based azomethine derivatives **2**, **4a-b** against cancer proteins. ADME/T analysis was performed to examine the drug properties of benzidine-based azomethine derivatives **2**, **4a-b**. The compounds **2**, **4a-b** are promising as potential anticancer drug candidates.

Highlights

- A novel benzidine-based azomethine derivate with a proposed new mechanism and two of its derivatives have been designed, synthesized and characterized by using spectroscopic techniques.
- The anticancer properties of the benzidine-based azomethine derivates were evaluated against two cancer cell lines (MDA-MB-231 human breast adenocarcinoma and DLD1 human colorectal adenocarcinoma cells).
- The molecular docking calculations were made to compare the biological activities of benzidine-based azomethine derivatives against cancer proteins. ADME/T analysis was performed to examine the drug properties of benzidine-based azomethine derivatives.
- The results showed that the benzidine-based azomethine derivates had a significant anti-proliferative effect especially against human breast cancer cell line,MDA-MB-231.

1. Introduction

Cancer refers to a collection of more than 200 different types of cancer disease. Cancer occurs by a series of mutations in specific genes in a cell, particularly controlling cell growth and division. This cell divides without stopping and spread into surrounding tissues. Cancer is the second leading cause of mortality worldwide, breast and colorectal cancers constitute the cancer types with the greatest frequency after lung cancer [1, 2]. There are many types of cancer treatment, including surgery, radiotherapy, and systemic therapy [3]. Chemotherapy is one of the most common treatment methods for cancer and may

be used in combination with other methods, such as surgery and radiation therapy. Since chemotherapeutic agents used to remove a tumor in a specific location of the body circulates throughout the body, they can carry a risk of side effects whose severity depending on the drug. Synthetizing novel chemotherapeutic agents having strong anti-cancer potential with minimum side effects is still a high necessity [4, 5] .

Benzidine (4,4'-diaminobiphenyl) is an aromatic amine compound containing a biphenyl scaffold and is a biologically and pharmacologically important skeleton. Benzidine derivatives have been widely used for the detection of blood and, as a starting material in dye production. Benzidine-based azo dyes are important and are widely used in industry [6].

Compounds containing azomethine groups are very stable and easily synthesized in a one-step condensation reaction between aldehydes and amines [7, 8]. Besides, they are also known as environmentally friendly compounds because water is the only byproduct in these reactions and complex purification is not required [9]. Moreover, such compounds have increased interest in these compounds due to their wide use in industry, in many fields of chemistry, medicine and pharmaceutical industry, making them widely used in different fields [10]. Among these applications, it came to the fore as bioactive substances due to the contribution of the azomethine group to bioactivity by interacting with certain regions in the cell structure and forming hydrogen bonds [11].

The azomethine derivatives are biologically active compounds in medicinal and biological applications as antibacterial [12–15], antimalarial [16–18], and anticancer [19–22], agents over the past few years. It has been reported in many studies that azomethine derivatives obtained from the reaction of various amines and aldehydes have anticancer activity.

It is seen in recent studies that theoretical studies are increasing its popularity quickly and reliably. Due to the developments in technology and the high accuracy of the results obtained from theoretical studies, theoretical studies have become very common [23, 25]. There are many programs and methods used in theoretical calculations. The best-known today is molecular docking calculations. In this study, cancer proteins used against benzidine-based azomethine derivatives **2**, **4a-b**: protein structure of MLK4 kinase domain (pdb ID: 4UYA) [26] and crystal structure of the BRCT repeat region from the breast cancer associated protein (pdb ID: 1JNX) [27].

The MLK4 protein used in this study demonstrates their tumor suppressor role, and kinases are tumor suppressors in many tumor types, including colon, lung, pancreatic and ovarian cancers [28, 29]. The C-terminal BRCT region of BRCA1, another protein, is a protein required for DNA repair, transcription regulation, and tumor suppressor functions [30]. There are two BRCT repeats that adopt similar structures in the BRCT region of human BRCA1 and are packaged together in an end-to-end arrangement [31–32]. False mutations that cause breast cancer occur at the interface between the two repeats and destabilize the structure. After molecular docking calculations, ADME/T calculations were made to examine the properties of benzidine-based azomethine derivatives **2**, **4a-b** as drugs.

Herein, we successfully synthesized in high yield three benzidine-based azomethine derivatives **2**, **4a-b** which were synthesized simply in a one-step condensation reaction between aldehydes (formaldehyde, benzaldehyde **3a** or *p*-nitrobenzaldehyde **3b**) and amine (benzidine (**1**)). According to our best knowledge, one of these compounds (the compound **2**) has been undetermined in the literature, and the other two compounds (the compounds **4a-b**) have not been studied in human colon cancer cells or human breast cancer cells as anti-cancer agents so for. Moreover, the chemical structure of the synthesized compounds was determined by NMR, FT-IR, and HRMS. The anticancer activities of these benzidine-based azomethine derivatives **2**, **4a-b** against human colon cancer cells (DLD1) and human breast cancer cells (MDA-MB-231) were investigated. The synthesized benzidine-based azomethine derivatives **2**, **4a-b** were found to exhibit good anticancer activity, especially against MDA-MB-231.

2. Result And Discussion

Synthesis and characterization of the compounds 2, 4a-b

Three benzidine-based azomethine derivatives **2**, **4a-b** were synthesized in good yields. The synthetic routes and synthesized compounds were shown in Scheme 1. Benzidine (**1**) which was commercially available was used as the starting material for the preparation of target compounds **2**, **4a-b**. Interestingly, treatment of benzidine (**1**) with an excess of formaldehyde (20 equiv.) in refluxing EtOH for 12 h afforded the compound **2** an excellent yield (98%). Scheme 2 shows the proposed reaction mechanism for the synthesis of the newly obtained compound **2.** As it is known, formaldehyde is a very reactive type of aldehyde. It is thought that imine is formed first in the reaction medium as a result of the rapid reaction of formaldehyde with free amine groups in the benzidine skeleton. As a result of the reaction of the formed imine group with EtOH, which was used as a solvent, the product **2** was obtained (Scheme 2). Synthesis of the compounds **4a-b** was achieved by the condensation of benzidine (**1**) with 2.1 equivalents of the appropriate aromatic aldehydes **3a-b** in refluxing EtOH according to a previously reported method [33, 34].

The reaction progress was monitored by TLC and when starting materials run out the reaction was confirmed. Chemical structures of newly the obtained compounds were characterized by NMR, IR, and as well as HRMS spectral analyses. The molecular weights, formula, melting point (m.p), appearance and yields of the benzidine-based azomethine derivatives are shown in Table 1.

Table 1
Some properties of the synthesized benzidine-based azomethine derivatives **2**, **4a-b**.

Compounds	Molecular Formula	Moleculer Weight (g/mol)	Color and Appearance	M.p ˚C	Yield (%)
2	$C_{24}H_{36}N_2O_4$	416,55	White powder	137–139	98
4a	$C_{26}H_{20}N_2$	360,45	Yellow powder	231–233	95
4b	$C_{26}H_{18}N_4O_4$	450,45	Brown powder	218–220	91

^{1}H NMR spectrum of the compound **2** (Fig. 1) having a symmetrical structure, consists of sets of signals appearing in aliphatic and aromatic region. The aromatic Ha protons are split into a doublet by the *ortho*- or 1,2- coupling with the Hb protons 7.45 ppm (J = 8.7 Hz, 4Ha). The Hb protons resonate as a doublet at 7.11 ppm, due to coupling with the Ha protons (J = 8.7 Hz, 4Hb). The Hc protons resonates as a singlet at 4.88 ppm (8H) due to the aliphatic -CH_2-units. Ethoxy protons (Hd and He) are resonate as quartet at 3.52 (q, J = 7.0 Hz, 8Hd) and triplet at 1.24 (t, J = 7.0 Hz, 12He) ppm, respectively. In addition, ^{13}C NMR spectrum of the compound **2** consists of sets of signals appearing in aliphatic and aromatic regions. The proton-decoupled ^{13}C NMR spectrum of compound **2** shows 7 carbon signals because of its symmetrical structure. The data matched very well with the structure of the molecule (Fig. 2).

The IR spectrum of the compound **2** exhibited characteristic absorptions bands at about 3091 cm^{-1}, 1388 cm^{-1}, 1100 cm^{-1}, 997 cm^{-1} and 817 cm^{-1}. The C–H stretching band was seen at 3091 cm^{-1}. The asymmetric C–C stretching band was also seen at 1388 cm^{-1}. The band located at 1100 cm^{-1} was assigned to the asymmetric ring vibration [35]. Moreover, the IR spectra of the compound **2** showed one characteristic band at 1330 cm^{-1} is known as the formation of the (C—N) band and one characteristic band at 1265 cm^{-1} is also known as the formation of the (C—O) band. The other band located at 1610 cm^{-1} was assigned to C=C stretching band [21, 34] (Fig. 3).

High-resolution mass spectrometry (HRMS) confirmed the constitution of the compound **2** (Fig. 4). The HRMS results demonstrated excellent agreement between the calculated mass (209.10787) and the obtained mass (209.10787) with the separation of $C_{10}H_{24}O_4$ atom group from the structure (m/z [(M-$C_{10}H_{24}O_4$) + H]$^+$).

Anticancer activity of the compounds 2, 4a-b

After successfully synthesized and characterized the three benzidine-based azomethine derivatives, named compounds **2, 4a-b**, we investigated whether these molecules had any anti-cancerogenic effects as anti-cancerogenic qualities of similar structures has previously been reported. We evaluated the antiproliferative action of these compounds in breast and colon cancer cell lines at five different concentrations (1, 10, 20, 50, 100 µM/mL) for 24 h. First, we tested 1-100 µM/mL benzidine-based

azomethine derivatives in the MDA-MB-231 breast cancer cell line. The number of breast cancers decreased compared to the control group in a dose-dependent manner in response to benzidine-based azomethine derivatives administration (Fig. 5). The compounds **2** and **4b** significantly decreased the number of breast cancer cells as low as 1 μM/mL. Among the three compounds examined, the compound **2** had the highest anti-proliferative effect and killed more than 50 % of the cells in response to 100 μM/mL. The compounds **4a-b** killed about 34 % and 30 %, respectively (Fig. 5).

As for DLD1 cells, the anti-proliferative actions of these three benzidine-based azomethine derivatives **2**, **4a-b** were less effective for this colon cancer cell line than that of for MDA-MB-231 cells. None of the compounds significantly killed the cells as low as 1–10 μM/mL concentrations compared to the control group. The compounds **2** and **4a** had similar anti-proliferative action and killed almost 38% of the cells in response to 100 μM/mL. The compound **4b** was less effective and killed only 20% of breast cancer cells (Fig. 6).

Cancer cells (DLD1, MDA-MB-231) were treated with increasing concentrations of benzidine-based azomethine derivatives **2**, **4a-b**. The compound **2** displayed the highest antiproliferative property among these three molecules and started to kill breast cancer cells as low as 1 μM/mL and killed colorectal cancer cells as low as 20 μM/mL. Starting at 20 μM/mL, the characteristic morphology of the cells also started to change in addition to decrease in the number of the cells in breast cancer cell line which could be clearly seen under a light microscope (Fig. 7).

In other words, exposure of cancer cell lines to these compounds, shrinkage and rounding of the cells were observed in which an indication of apoptosis, in our opinion. Likewise, exposure of DLD1 colorectal cancer cell line to 20 μM/mL the compound **2**, similar morphological changes associated with the apoptosis was determined as seen in the breast cancer cells (Fig. 8).

Molecular docking calculations

It is used to compare the activities of the molecules **2**, **4a-b** against cancer proteins by theoretical calculations. In molecular docking calculations, which are most commonly used in these calculations, it is seen that the values closest to the results obtained as a result of experimental processes have a great harmony [25, 37]. Many parameters are calculated from molecular docking calculations. Among these calculated parameters, the most important parameter that determines the activity is the docking score. The numerical value of this parameter is expected to be negative. The more negative value the molecule is thought to have higher activity than other molecules. The most important factor affecting the molecule to have a more negative value is the chemical interaction [25]. It should be well known that the more the molecule interacts with the protein, the higher the docking score. These interactions have many interactions such as hydrogen bonds, polar and hydrophobic interactions, π-π and halogen [37–43].

In comparing the activities of the molecules **2**, **4a-b**, it is not sufficient to examine the docking score parameter only. It is necessary to examine other calculated parameters. All parameters obtained from molecular docking calculations are visualized in Table 2. Some of these other parameters are Glide

hbond, Glide evdw, and Glide ecoul parameters. These parameters are the chemical interactions of molecules with cancer proteins [38]. The interaction of the molecule **2** with the highest activity is given in Figs. 9–10. Other remaining parameters are Glide emodel, Glide energy, Glide einternal, and Glide posenum parameters. These parameters provide numerical information for the interaction of molecules with cancer proteins [39–40].

Table 2
Numerical values of the docking parameters of molecules 2, 4a-b against proteins

Breast cancer	**Compound 2**	**Compound 4a**	**Compound 4b**
Docking Score	-3.43	-3.37	-3.27
Glide ligand efficiency	-0.10	-0.12	-0.10
Glide hbond	-0.16	-0.21	-0.13
Glide evdw	-31.02	-30.51	-34.22
Glide ecoul	-6.64	-2.04	-2.03
Glide emodel	-43.95	-37.83	-41.83
Glide energy	-37.67	-32.55	-36.25
Glide einternal	2.67	4.14	2.91
Glide posenum	90	43	383
Colon cancer	**Compound 2**	**Compound 4a**	**Compound 4b**
Docking Score	-4.91	-4.83	-4.40
Glide ligand efficiency	-0.14	-0.17	-0.13
Glide hbond	-0.24	0.00	0.00
Glide evdw	-37.58	-34.33	-39.59
Glide ecoul	-6.48	0.56	-0.37
Glide emodel	-51.87	-42.35	-49.05
Glide energy	-44.06	-33.76	-39.96
Glide einternal	12.74	5.21	5.55
Glide posenum	95	307	132

Comparison of the activities of the molecules **2**, **4a-b** against cancer proteins was made. It is not enough for a molecule to be a drug only if its activity is high. How these molecules act in human metabolism is very important in order to become drugs. Because when molecules enter human metabolism and cause toxic effect, it can cause human death [41]. Therefore, ADME/T analysis of molecules is performed. With

this analysis, the route of entry of molecules in human metabolism, their interaction, excretion by human metabolism, and the toxic effects they cause have been examined in detail [42, 43]. All calculated ADME/T parameters are given in Table 3.

Table 3
ADME properties of the molecules 2, 4a-b.

	2	4a	4b	Referance Range
mol_MW	417	360	450	130–725
dipole (D)	2.5	3.2	6.7	1.0-12.5
SASA	867	727	806	300–1000
FOSA	620	45	45	0-750
FISA	8	30	233	7-330
PISA	239	652	528	0-450
WPSA	0	0	0	0-175
volume (A^3)	1525	1279	1429	500–2000
donorHB	0	0	0	0–6
accptHB	8.8	2	4	2.0–20.0
glob (Sphere = 1)	0.7	0.8	0.8	0.75–0.95
QPpolrz (A^3)	47.5	46.7	50.3	13.0–70.0
QPlogPC16	14.6	15.0	17.1	4.0–18.0
QPlogPoct	19.4	16.7	20.0	8.0–35.0
QPlogPw	8.8	6.5	8.8	4.0–45.0
QPlogPo/w	5.2	7.2	5.7	-2.0-6.5
QPlogS	-5.6	-7.8	-7.9	-6.5-0.5
CIQPlogS	-4.6	-7.2	-8.2	-6.5-0.5
QPlogHERG	-6.9	-8.1	-7.9	(corcern below − 5)
QPPCaco (nm/sec)	8278	5144	61	*
QPlogBB	-0.4	-0.2	-2.7	-3.0-1.2
QPPMDCK (nm/sec)	4859	2905	24	*
QPlogKp	0.6	0.9	-3.1	Kp in cm/hr
IP (ev)	9.5	8.6	9.1	7.9–10.5
EA (eV)	0.1	0.9	2.5	-0.9-1.7
#metab	6	0	2	1–8

	2	4a	4b	Referance Range
QPlogKhsa	0.1	1.5	1.3	-1.5-1.5
Human Oral Absorption	3	1	1	-
Percent Human Oral Absorption	100	100	79	**
PSA	42	22	116	7-200
RuleOfFive	1	1	1	Maximum is 4
RuleOfThree	0	1	1	Maximum is 3
Jm	4.3	0.0	0.0	-

* <25 is poor and > 500 is great, ** <25% is poor and > 80% is high.
As a result of this investigation, many parameters were found. One of these parameters found is the molar mass (mol_MW). Because it is desired that the mole cult is neither too little nor too much [37]. On the other hand, it is desired that the dipole moment (dipole (D)) of the molecules should be neither too little nor too much [38]. Another parameter is the number of hydrogen bonds (donorHB and accptHB) taken or given between molecules and proteins. There are many parameters such as the numerical information of the passage of molecules through the blood-intestine (QPPCaco) and blood-brain (QPPMDCK) barriers [39, 40]. It is seen that the compounds **2** and **4a** are not suitable for these parameters. Parameters such as RuleOfFive and RuleOfThree are the parameters that decide whether the molecules are suitable for use as drugs because these parameters are made up of many parameters [41–43]. Therefore, the numerical value of the RuleOfFive and RuleOfThree parameters is expected to be zero. When the parameters contained in these parameters do not meet the required conditions, a number increases for each parameter. Therefore, it is considered appropriate to be used as a medicine if all the parameters they contain provide the necessary conditions.

3. Conclusions

A novel benzidine-based azomethine derivative **2** having a proposed new mechanism and its other two derivatives **4a-b** have been successfully synthesized in high yields by reaction of benzidine (**1**) with formaldehyde, benzaldehyde **3a** or nitrobenzaldehyde **3b**. The structural characterization of the compounds **2**, **4a-b** has been evaluated by using NMR, FT-IR, and HRMS. Ultimately, the synthesized compounds **2**, **4a-b** were evaluated for their anticancer activities against human breast cancer cells (MDA-MB-231) and human colon cancer cells (DLD1). They have shown anticancer potential against these cancer cells. The results showed that the benzidine-based azomethine derivatives **2**, **4a-b** had a significant effect against the human breast cancer cell line (MDA-MB-231). The compound **2** had the highest anti-proliferative effect against (MDA-MB-231) and killed more than 50% of the cells in response to 100 µM/mL. The compounds **4a-b** killed about 34% and 30%, respectively. The results of this research encourage us to develop other similar related compounds and test them for a wide range of anticancer

activity. However, it is seen that there is a great agreement between the theoretical studies and the experimental results. According to the results of molecular docking, it is seen that it is the compound **2** with − 3.43 against breast cancer protein and − 4.91 against colon cancer protein. According to the ADME / T results performed afterwards, although the molecules **2**, **4a-b** have problems in some parameters, it is thought that there will be no problem in the use of more detailed *in vivo* and *in vitro* experiments to be carried out in the future. Although theoretical calculations will guide future studies, it is impossible to predict what effects the molecules will have for different human metabolism.

4. Experimental Section

Synthesis of the compound 2

All commercially available chemicals were obtained from Sigma-Aldrich and used without further purification. To a 100 mL one-necked round-bottomed flask equipped with a condenser were added benzidine (**1**) (0.5 g, 2.71 mmol) and ethanol (50 mL). To the above solution was added formaldehyde solution (54.28 mmol, 1.63 g, 20 equiv), and the reaction mixture was refluxed for 12 h and monitored by TLC. After complete consumption of benzidine (**1**), the reaction mixture was concentrated under reduced pressure. The mixture was then cooled to room temperature. Upon cooling the resulting reaction solution to ambient temperature, white solids precipitated from solution, the solid product was filtered and washed with cold methanol and then dried in vacuo to give the compound (**2)** (yield, 98%). *N^4,N^4,$N^{4'}$,$N^{4'}$-Tetrakis(ethoxymethyl)-[1,1'-biphenyl]-4,4'-diamine* (**2**): Mp: 137–139°C IR (cm^{-1}): 3091, 3019, 1979, 2932, 2879, 2877, 1610, 1505, 1422, 1388, 1367, 1330, 1265, 1203, 1161, 1100, 1058, 1034, 997, 966, 897, 836, 817, 764, 751, 677, 631. ^{1}H NMR (400 MHz, $CDCl_3$): δ 7.45 (d, J = 8.7 Hz, 4H), 7.11 (d, J = 8.7 Hz, 4H), 4.88 (s, 8H), 3.52 (q, J = 7.0 Hz, 8H), 1.24 (t, J = 7.0 Hz, 12H). ^{13}C NMR (100 MHz, $CDCl_3$): δ 145.60, 132.60, 127.09, 114.98, 82.76, 62.36, 15.16. HRMS (Q-TOF): m/z $[(M\text{-}C_{10}H_{24}O_4) + H]^+$ calcd. for $C_{14}H_{13}N_2$: 209.10787, found: 209.10787.

General procedure for synthesis of the compounds 4a-b

Benzidine (**1**) (1.000 mmol) and aromatic aldehydes **3a** or **3b** (2.100 mmol) were dissolved in EtOH, and the resulting reaction mixture was heated at the refluxed temperature for 12 h and monitored by TLC. After complete consumption of aromatic aldehyde, the reaction mixture was concentrated under reduced pressure. The mixture was then cooled to room temperature. Upon cooling the resulting reaction solution to ambient temperature, crystals precipitated from solution, the solid product was filtered and washed with cold methanol and then dried *in vacuo* to give the compound **4a-b** [34, 44].

(1E,1'E)-N,N'-([1,1'-biphenyl]-4,4'-diyl)bis(1-phenylmethanimine) (**4a**): Mp: 231–233°C. ^{1}H NMR (400 MHz, $CDCl_3$): δ 8.53 (s, 2H, CH = N), 7.98–7.89 (m, 4H), 7.71–7.63 (m, 4H), 7.53–7.46 (m, 6H), 7.36–7.29 (m, 4H).

(1E,1'E)-N,N'-([1,1'-biphenyl]-4,4'-diyl)bis(1-(4-nitrophenyl)methanimine) (**4b**): Mp: 218–220°C. ^{1}H NMR (400 MHz, $CDCl_3$): δ 8.62 (s, 2H), 8.33 (d, J = 8.8 Hz, 6H), 8.09 (d, J = 8.8 Hz, 2H), 7.61 (d, J = 8.6 Hz, 4H), 7.33 (d, J = 8.6 Hz, 4H).

Anticancer activity of the compounds 2, 4a-b

Cell culture

MDA-MB-231 breast cancerand DLD1 colorectal cancer cell lines were maintained in Dulbecco's Modified Eagle Medium (DMEM) containing 10% fetal bovine serum (FBS) and 1% Penicillin-Streptomycin. Cancer cell lines were maintained at 37°C and 5% CO_2 in an incubator.

Measurement of cell survival

Cancer cells were seeded in 96-well plates at a density of 0.5 x 10^4 in 200 µl culture medium and incubated at 37°C and 5% CO_2 until the cells were grown to reach about 70% confluency before chemical treatments. Then, the cells were treated with different concentrations of the compound **2** for 24 hrs. Cell survival was determined using the Eco-Tech CVDK-8 Cell Viability kit (EcoTech Biotechnology, Turkey) according to the manufacturer's recommendations. The assay is based on the reduction of WST-8 (2-(2-methoxy-4-nitrophenyl)-3-(4-nitrophenyl)-5-(2,4-disulfophenyl)-2*H*-tetrazolium, monosodium salt). As a result of WST-8 bio-reduction, the amount of yellow-colored formazan is produced in the culture medium and this is directly proportional to the number of living cells. The absorbance of the medium in each well was measured at 450 nm via a spectrophotometer.

Statistical analysis

The data set was created by transferring the absorbance values and folding time calculation results of the wells to IBM SPSS 20.0 software. The variance homogeneity test was applied according to the results obtained by applying the Shapiro-Wilk normality test to the created data set and $p < 0.05$ was considered significant. One-Way ANOVA test was applied to all the data and the appropriate Post-Hoc test was selected according to the variance homogeneity test results and $p < 0.05$ was considered significant.

Instrumentation

^{1}H NMR spectra were recorded on a Bruker Ultrashield Plus Biospin spectrometer at 400 MHz. NMR chemical shifts were determined relative to internal standard TMS at δ 0.0 ppm. The chemical shifts (δ) are reported in ppm, and coupling constants (J) are in Hertz (Hz). Melting Points (M.p) were recorded on a Stuart melting point SMP30 device and are uncorrected. FTIR spectra were recorded using a Perkin Elmer Frontier FT-IR spectrophotometer. Mass spectra were recorded on an Agilent Technologies 6530 Accurate-Mass Q-TOF-LC/MS. The absorbance of the cell culture medium was measured via an ELx800 BioTek spectrophotometer.

Molecular docking calculations

Molecular docking calculations are the common method used to compare the activities of molecules. In this method, the interactions of molecules with proteins are examined. These calculations are made using the Maestro Molecular modeling platform (version 12.2) by Schrödinger [45]. For these calculations, it is necessary to prepare both proteins and molecules, which consists of many stages. It is the preparation process of the proteins studied in the first stage. At this stage, active sites of proteins are determined. All proteins in this active region were given freedom of movement, because the molecules were easier to interact with the proteins. At this stage, the protein preparation module [46] is used. The next stage is the preparation of molecules for calculations. In this process, all conformers of the molecules are prepared. For the interaction of proteins and molecules, each structure is tested one by one, in an attempt to find the most stable interaction pose. the LigPrep module [47] is used in the calculations of this stage. In the next step, the interactions of molecules with proteins are made. At this stage, calculations are made with The Glide ligand docking module [48] for calculations. In these calculations, the preparation of molecules and proteins is calculated by the OPLS3e method. In the next stage, the properties of molecules to be drugs are examined. This analysis is performed to predict the actions of drug molecules in human metabolism. These calculations are calculated by The Qik-prop module [49] of the Schrödinger software.

Declarations

Declaration of Competing Interest

The authors declare that they have no known competing financial interests or personal relationships that could have appeared to influence the work reported in this paper.

References

1. Ashour HF, Abou-Zeid LA, El-Sayed MA, Selim KB (2020) Eur J Med Chem 189:112062.
2. Muskinja JM, Burmudzija AZ, Baskic DD, Popovic SL, Todorovic DV, Zaric MM, Ratkovic ZR (2019) Med Chem Res 28:279.-291.
3. Riaz S, Iqbal M, Ullah R, Zahra R, Chotana GA, Faisal A, Saleem RSZ (2019) Bioorg Chem 87:123-135.
4. Farghaly TA, Masaret GS, Muhammad ZA, Harras MF (2020) Bioorganic Chemistry 98.
5. Ngameni B, Cedric K, Mbaveng AT, Erdogan M, Simo I, Kuete V, Dastan A (2021) Bioorg Med Chem Lett 35.
6. Amer YOB, El-Daghare, R.N., Hammouda, A.N., ElFerjani, R.M. and Elmagbari, F.M (2020) Open Journal of Inorganic Chemistry 10:6-14.
7. Qin WL, Long S, Panunzio M, Biondi S (2013) Molecules 18:12264-12289.
8. Xin Y, Yuan JY (2012) Polym Chem-Uk 3(11):3045-3055.
9. Petrus ML, Bouwer RKM, Lafont U, Athanasopoulos S, Greenham NC, Dingemans TJ (2014) J Mater Chem A 2:9474-9477.

10. Krzysztof Sztanke AM, Anna Osinka, Małgorzata Sztanke (2013) Bioorg Med Chem 21:3648-3666.
11. Venugopala KN, Jayashree BS (2003) Indian J Heterocy Ch 12:307-310.
12. Anush SM, Vishalakshi B, Kalluraya B, Manju N (2018) Int J Biol Macromol 119: 446-452.
13. Cleiton M. da Silva CMdSLdS, Luzia V.Modolo, Rosemeire B.Alves, Maria A.de Resende, Cleide V.B.Martins, Ângelo de Fátima (2011) Journal of Advanced Research 2:1-8.
14. Joseph J, Nagashri K, Rani GAB (2013) J Saudi Chem Soc 17:285-294.
15. Lapasam A, Dkhar L, Joshi N, Poluri KM, Kollipara MR (2019) Inorg Chim Acta 484:255-263.
16. Dhar DN, Taploo CL (1982) J Sci Ind Res India 41:501-506.
17. Harpstrite SE, Collins SD, Oksman A, Goldberg DE, Sharma V (2008) Med Chem 4:392-395.
18. Rathelot P, Vanelle P, Gasquet M, Delmas F, Crozet MP, Timondavid P, Maldonado J (1995) Eur J Med Chem 30:503-508.
19. Miri R, Razzaghi-asl N, Mohammadi MK (2013) J Mol Model19:727-735.
20. Modi JD, Sabnis SS, Deliwala CV (1970) J Med Chem 13:935.
21. Uddin N, Rashid F, Ali S, Tirmizi SA, Ahmad I, Zaib S, Zubair M, Diaconescu PL, Tahir MN, Iqbal J *Haider A (2020) J Biomol Struct Dyn 38*:3246-3259.
22. Wang Y, Pigeon P, McGlinchey MJ, Top S, Jaouen G (2017) J Organomet Chem 829:108-115.
23. Gürdere, M. B., Budak, Y., Kocyigit, U. M., Taslimi, P., Tüzün, B., & Ceylan, M. (2021). ADME properties, bioactivity and molecular docking studies of 4-amino-chalcone derivatives: new analogues for the treatment of Alzheimer, glaucoma and epileptic diseases. In Silico Pharmacology, 9(1), 1-11.
24. Gezegen, H., Gürdere, M. B., Dinçer, A., Özbek, O., Koçyiğit, Ü. M., Taslimi, P., ... & Ceylan, M. (2021). Synthesis, molecular docking, and biological activities of new cyanopyridine derivatives containing phenylurea. Archiv der Pharmazie, 354(4), 2000334.
25. Bilgiçli, A. T., Genc Bilgicli, H., Hepokur, C., Tüzün, B., Günsel, A., Zengin, M., & Yarasir, M. N. (2021). Synthesis of (4R)-2-(3-hydroxyphenyl) thiazolidine-4-carboxylic acid substituted phthalocyanines: Anticancer activity on different cancer cell lines and molecular docking studies. Applied Organometallic Chemistry, e6242.
26. Marusiak, A. A., Stephenson, N. L., Baik, H., Trotter, E. W., Li, Y., Blyth, K., ... & Brognard, J. (2016). Recurrent MLK4 loss-of-function mutations suppress JNK signaling to promote colon tumorigenesis. Cancer research, 76(3), 724-735.
27. Williams, R. S., Green, R., & Glover, J. M. (2001). Crystal structure of the BRCT repeat region from the breast cancer-associated protein BRCA1. Nature structural biology, 8(10), 838-842.
28. Kennedy, N. J., & Davis, R. J. (2003). Role of JNK in tumor development. Cell cycle (Georgetown, Tex.), 2(3), 199-201.
29. Whitmarsh, A. J., & Davis, R. J. (2007). Role of mitogen-activated protein kinase kinase 4 in cancer. Oncogene, 26(22), 3172-3184.
30. Miki, Y., Swensen, J., Shattuck-Eidens, D., Futreal, P. A., Harshman, K., Tavtigian, S., ... & Ding, W. (1994). A strong candidate for the breast and ovarian cancer susceptibility gene BRCA1. Science,

266(5182), 66-71.

31. Futreal, P. A., Liu, Q., Shattuck-Eidens, D., Cochran, C., Harshman, K., Tavtigian, S., ... & Miki, Y. (1994). BRCA1 mutations in primary breast and ovarian carcinomas. Science, 266(5182), 120-122.
32. Friedman, L. S., Ostermeyer, E. A., Szabo, C. I., Dowd, P., Lynch, E. D., Rowell, S. E., & King, M. C. (1994). Confirmation of BRCA1 by analysis of germline mutations linked to breast and ovarian cancer in ten families. Nature genetics, 8(4), 399-404.
33. 24. Iqbal A, Siddiqui HL, Ashraf CM, Bukhari MH, Akram CM (2007) Chem Pharm Bull55:1070-1072.
34. Mutahir S, Khan MA, Khan IU, Yar M, Ashraf M, Tariq S, Ye RL, Zhou BJ (2017) Eur J Med Chem 134:406-414.
35. Wang GB, Chang JC (1994) Syn React Inorg Met 24:1091-1097.
36. Türkan, F., Taslimi, P., Cabir, B., Ağırtaş, M. S., Erden, Y., Celebioglu, H. U., ... & Gulcin, I. (2021). Co and Zn Metal Phthalocyanines with Bulky Substituents: Anticancer, Antibacterial Activities and Their Inhibitory Effects on Some Metabolic Enzymes with Molecular Docking Studies. Polycyclic Aromatic Compounds, 1-13.
37. Aktaş, A., Tüzün, B., Aslan, R., Sayin, K., & Ataseven, H. (2020). New anti-viral drugs for the treatment of COVID-19 instead of favipiravir. Journal of Biomolecular Structure and Dynamics, 1-11.
38. Aktaş, A., Tüzün, B., Taşkın Kafa H.A., Sayin, K., & Ataseven, H. (2020). clarification of interaction mechanism of arbidol with covid-19 and investigation of the inhibition activity analogues against covid-19, Bratislava Medical Journal-Bratislavske Lekarske Listy, 121(10) 705-711.
39. Gedikli M.A., Tuzun B., Aktas A., Sayin K., Ataseven H., (2021) Are clarithromycin, azithromycin and their analogues effective in the treatment of COVID19?. Bratislavske Lekarske Listy, 122(2) 101-110. https://doi.org/10.4149/BLL_2021_015
40. Çetiner E., Sayin K., Tüzün B., Ataseven H., (2021) Could Boron-Containing Compounds (BCCs) be effective against SARS-CoV-2 as Anti-Viral Agent? Bratislavske lekarske listy 122(4) https://doi.org/10.4149/BLL_2021_44
41. Gedikli M.A., Tuzun B., Sayin K., Ataseven H., (2021) Determination of inhibitor activity of drugs against the COVID-19, Bratislavske lekarske listy 122(7) https://doi.org/10.4149/BLL_2021_81
42. Tüzün B., Nasibova T., Garaev E., Sayın K., Ataseven H. (2021) Could Alkaloids Be Effective In The Treatment of COVID-19? Bratislava Medical Journal, 122(9), https://doi.org/10.4149/BLL_2021_108
43. Ataseven H., Sayın K., Tüzün B., Gedikli M.A., (2021) Could boron compounds be effective against SARS-CoV-2? 122(10) https://doi.org/10.4149/BLL_2021_121
44. Gobel A, Leibeling G, Rudolph M, Imhof W (2003) Organometallics 22:759-768.
45. Schrodinger, L. (2019). Small-Molecule Drug Discovery Suite 2019-4
46. Schrödinger Release 2019-4: Protein Preparation Wizard; Epik, Schrödinger, LLC, New York, NY, 2016; Impact, Schrödinger, LLC, New York, NY, 2016; Prime, Schrödinger, LLC, New York, NY, 2019.
47. Schrödinger Release 2019-4: LigPrep, Schrödinger, LLC, New York, NY, 2019.
48. Schrödinger Release 2020-1: QikProp, Schrödinger, LLC, New York, NY, 2020.

49. Tüzün, B. Examination of anti-oxidant properties and molecular docking parameters of some compounds in human body. Turkish Computational and Theoretical Chemistry, 4(2), 76-87.

Figures

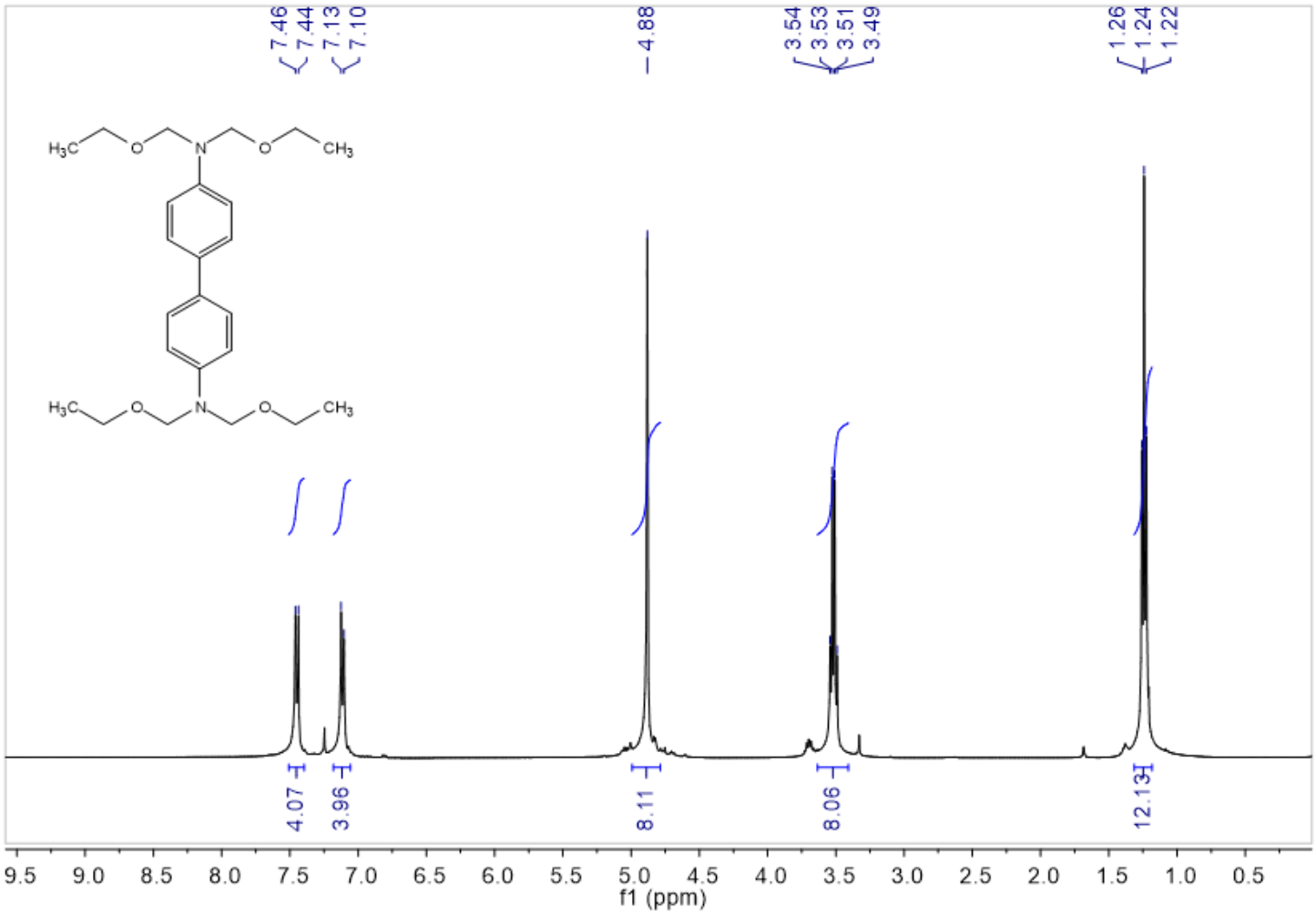

Figure 1

1H-NMR (400 MHz, CDCl3) spectrum of the compound 2.

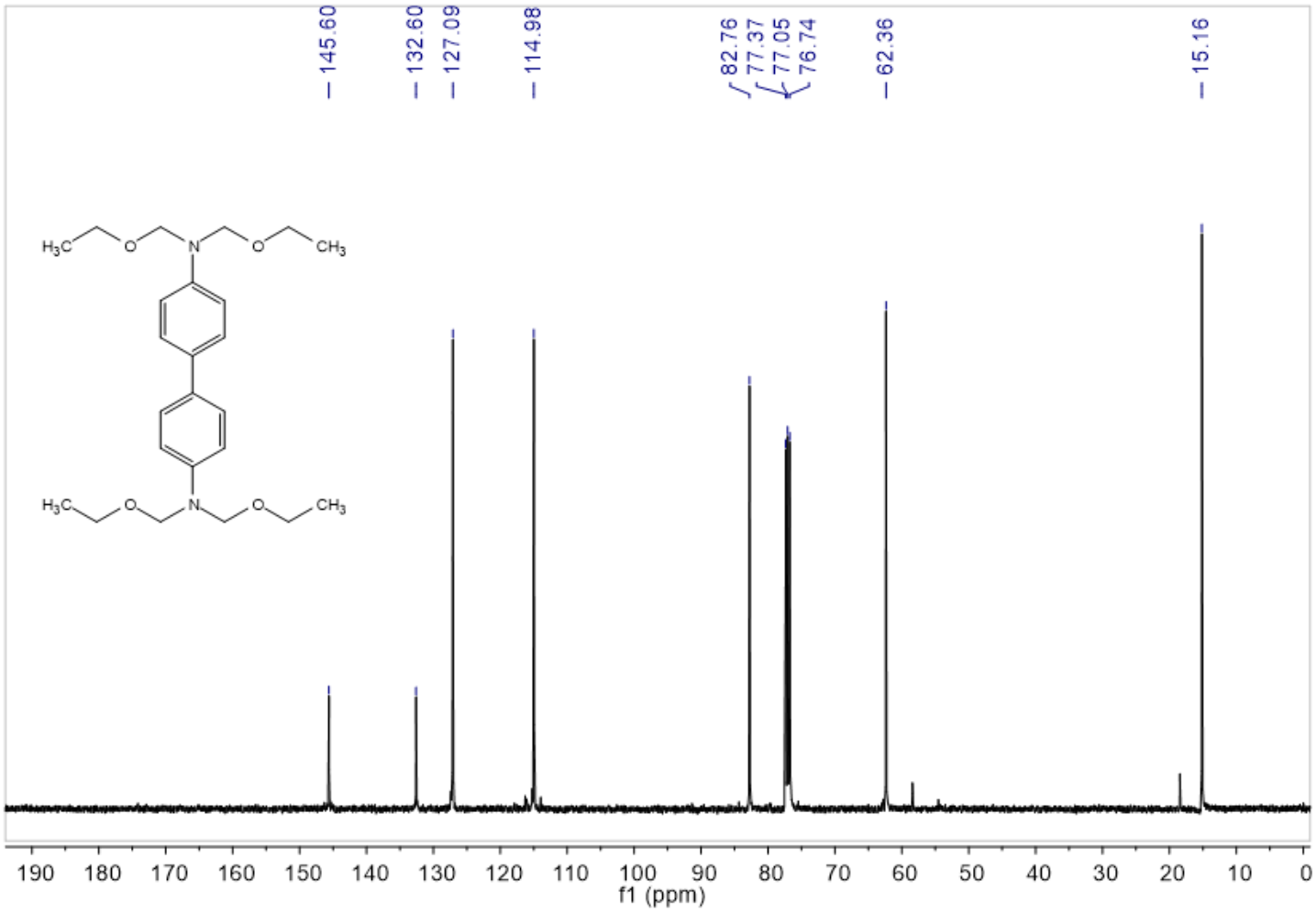

Figure 2

13C-NMR (100 MHz, CDCl3) spectrum of the compound 2.

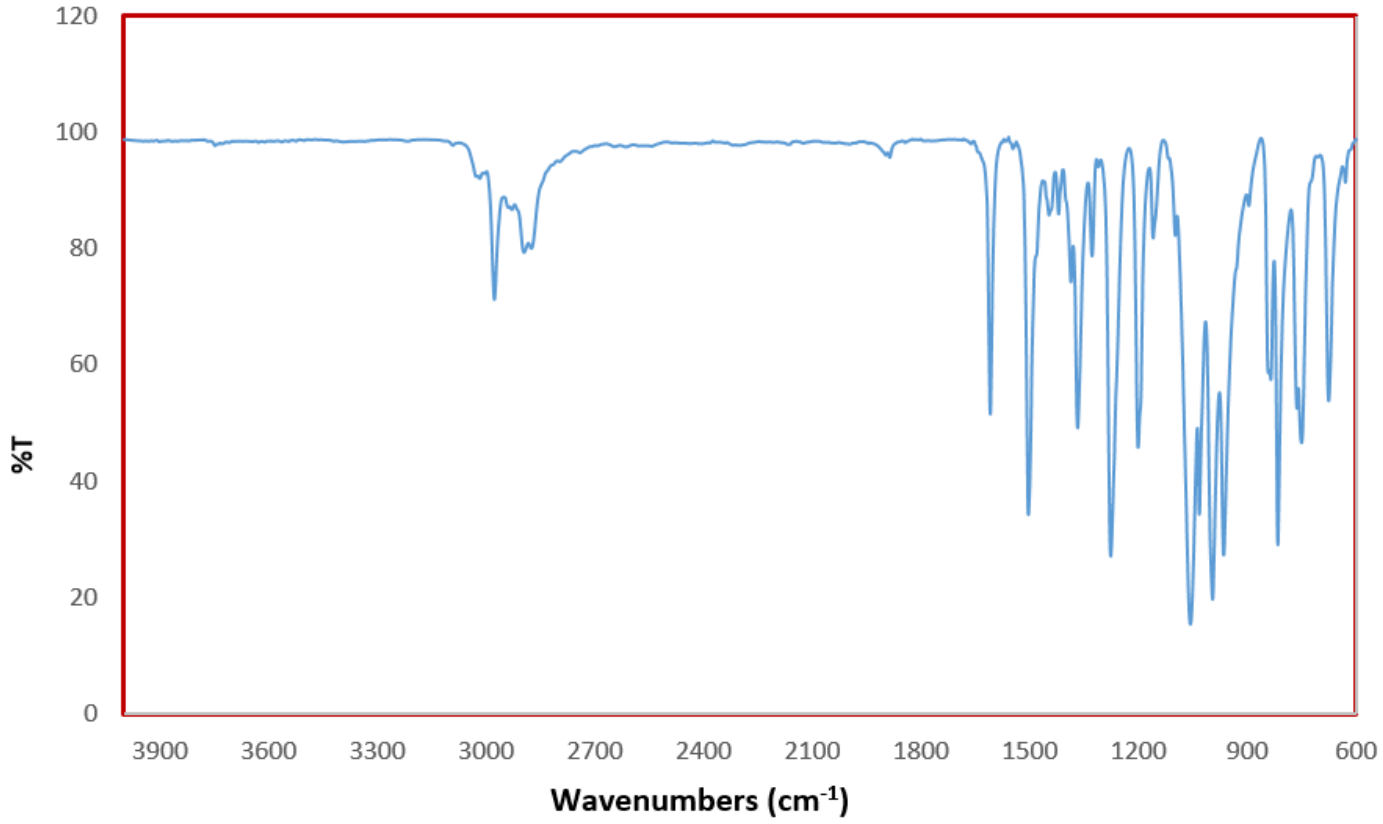

Figure 3

IR spectrum of the compound 2.

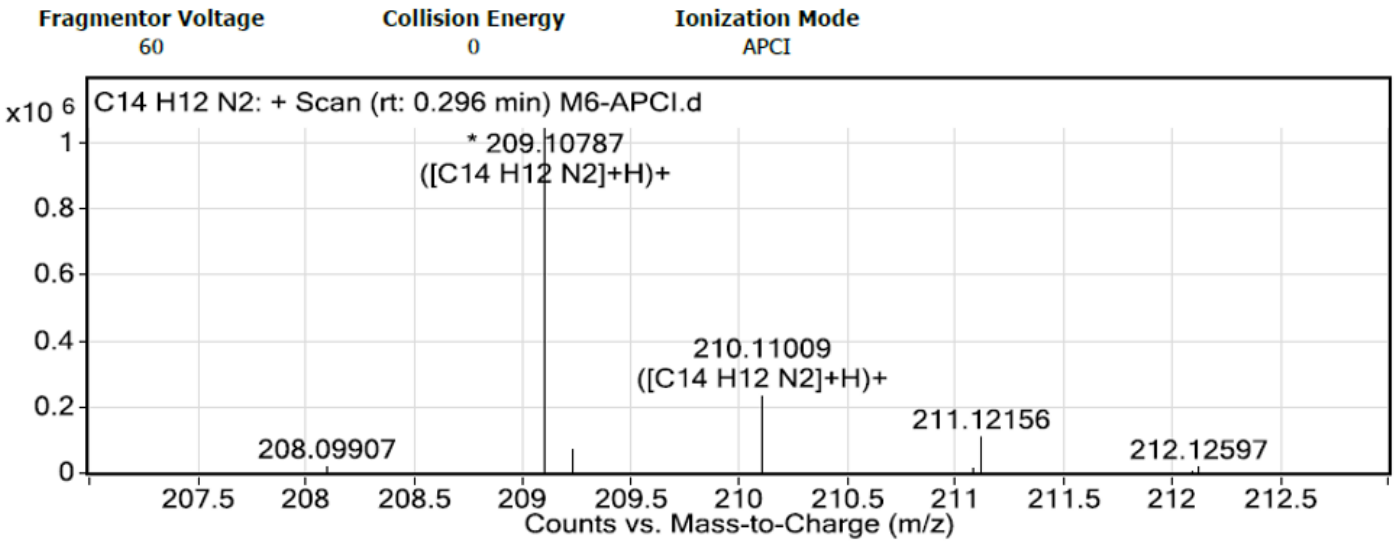

Figure 4

HRMS spectrum of the compound 2.

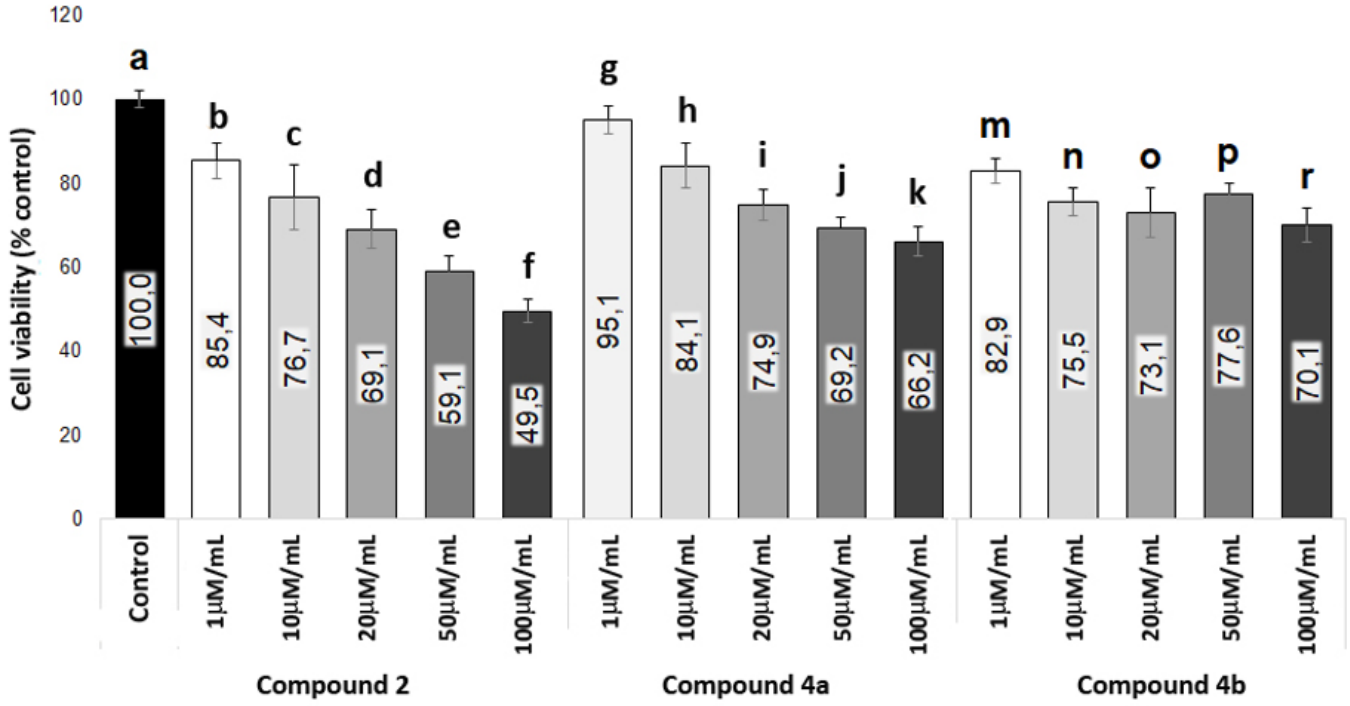

Figure 5

The MDA-MB-231 breast cancer cells were treated with 1-100 µg/mL. Benzidine-based azomethine derivatives 2, 4a-b for 24 hrs and relative survival fraction was determined. Error bars represent one standard deviation from the mean. One-Way ANOVA; p2, 4a, 4b<0.001. PostHoc Tamhane's T2; pad, ae, af, be, ai, aj, ak, gi, gj, gk, bf, am, an, ap, ar<0.001, pab, ac, bd, cf, df, hk, ao<0.01, pce, ef, ah, hj, mr<0.05. PostHoc Bonferroni; pjp<0.01, pej, ep, bg, gm, fk, fr<0.001. At least three independent experiments were performed.

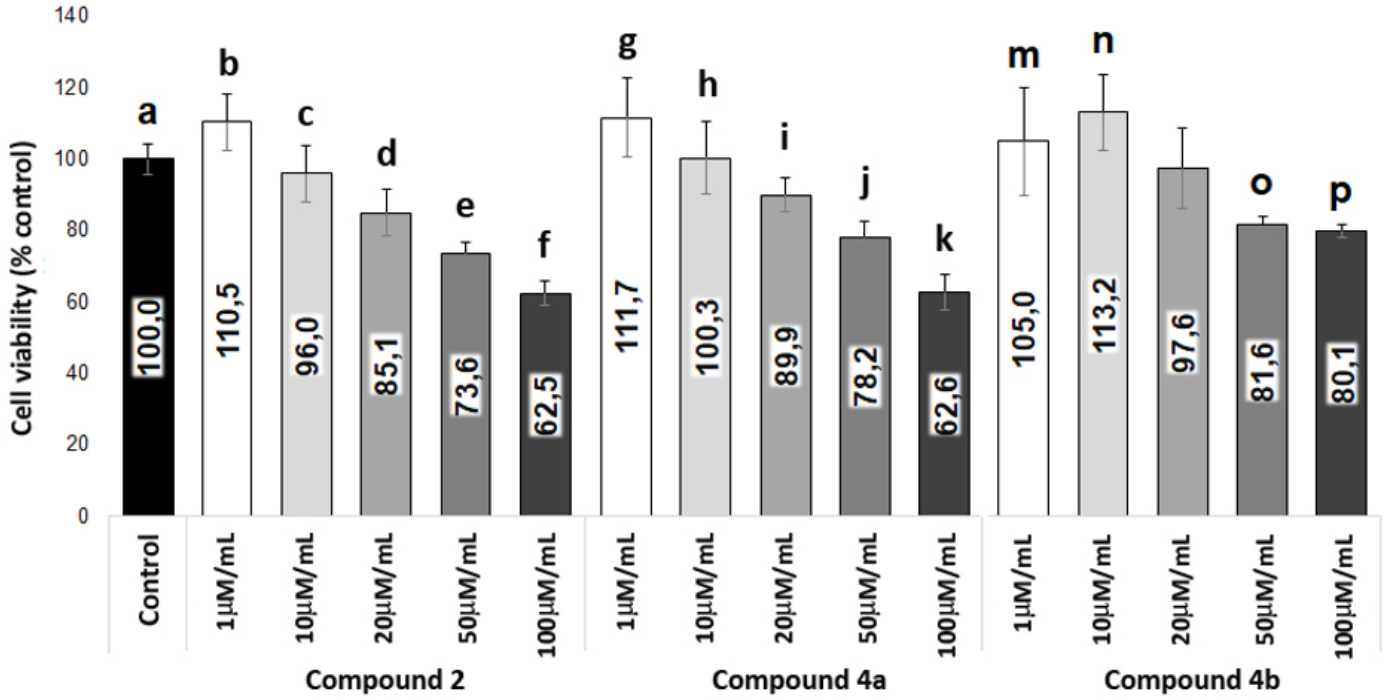

Figure 6

The DLD1 colon cancer cells were treated with 1-100 mg/mL benzidine-based azomethine derivatives 2, 4a-b for 24 hrs and relative survival fraction was determined. Error bars represent one standard deviation from the mean One-Way ANOVA; p2, 4a, 4b<0.001. PostHoc Tamhane's T2: pae, af, bd, bf, cf, aj, ak, gk, hk, ik, jk, am, an<0.001, pcd, ce, df, gj, no, np<0.01, pgi, hj, mo, mp<0.05. PostHoc Bonferroni; pcn, eo<0.05, pej<0.01, pfp, kp<0.001. At least three independent experiments were done.

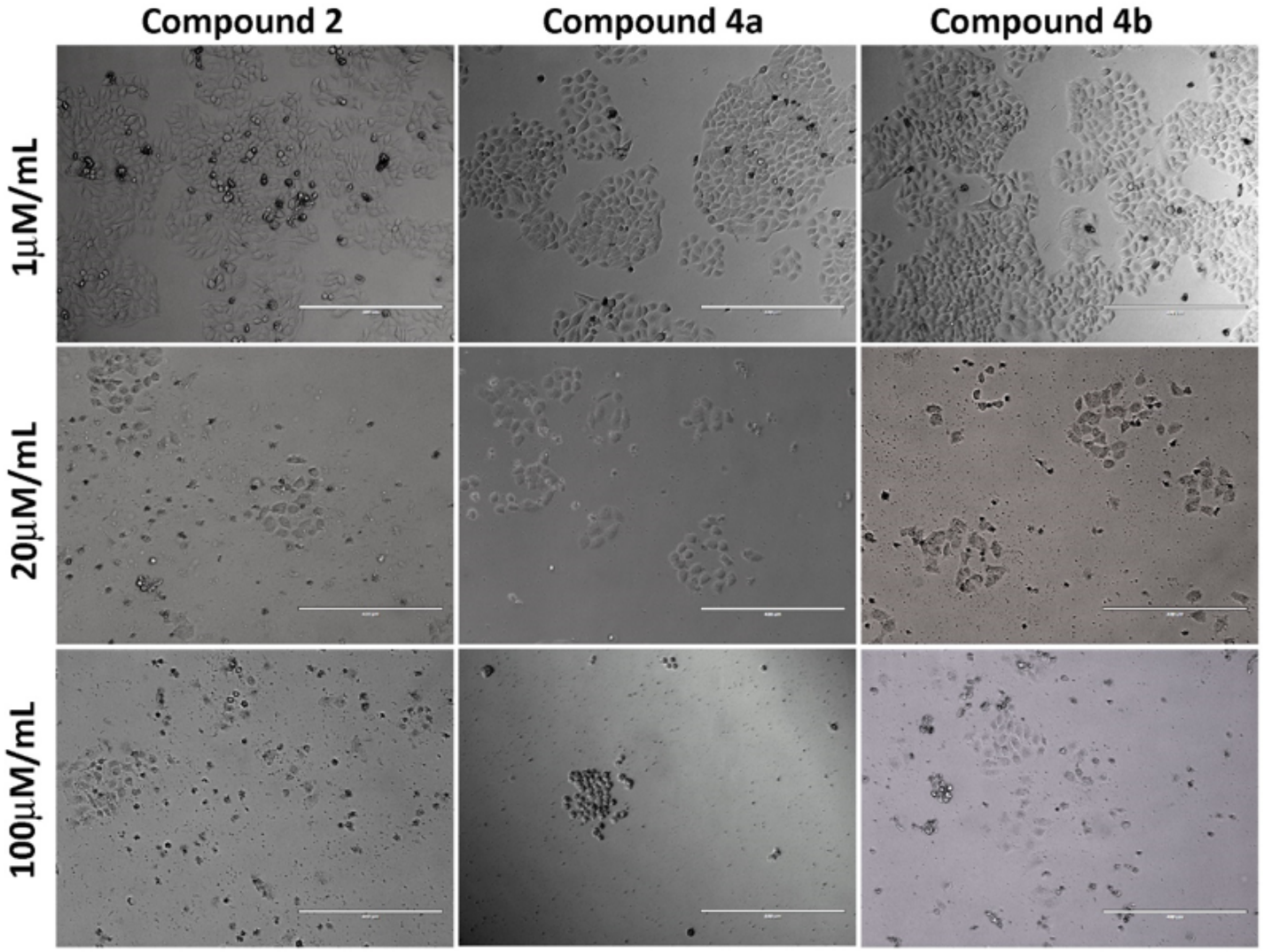

Figure 7

Light microscopy images of benzidine-based azomethine derivatives 2, 4a-b treated breast cancer cells (MDA-MB-231) for 24 hrs. At least three independent experiments were performed and representative images were shown. Scale bar: 400 μm.

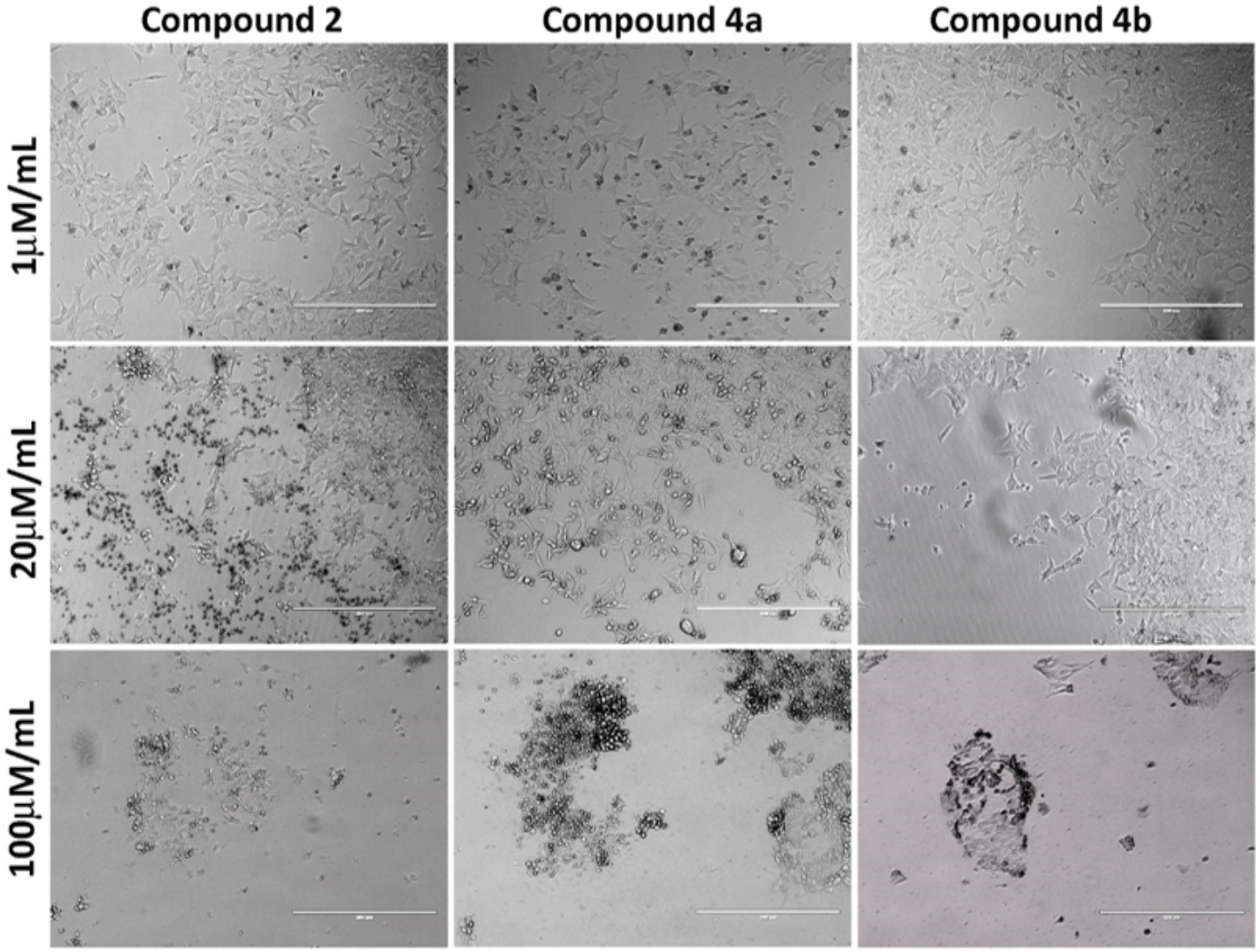

Figure 8

Light microscopy images of benzidine-based azomethine derivatives 2, 4a-b treated colon cancer cells (DLD) for 24 hrs. At least three independent experiments were performed and representative images were shown. Scale bar: 400 µm.

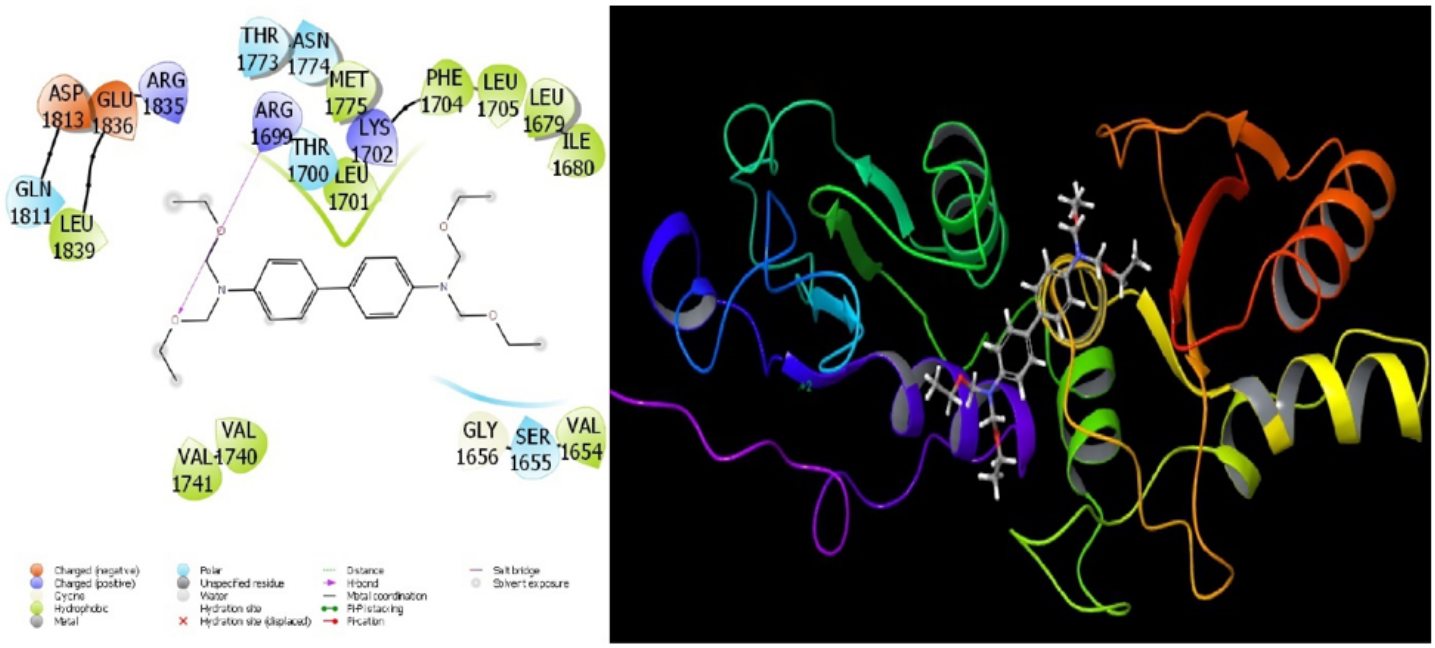

Figure 9

Presentation interactions of the compound 2 with breast cancer.

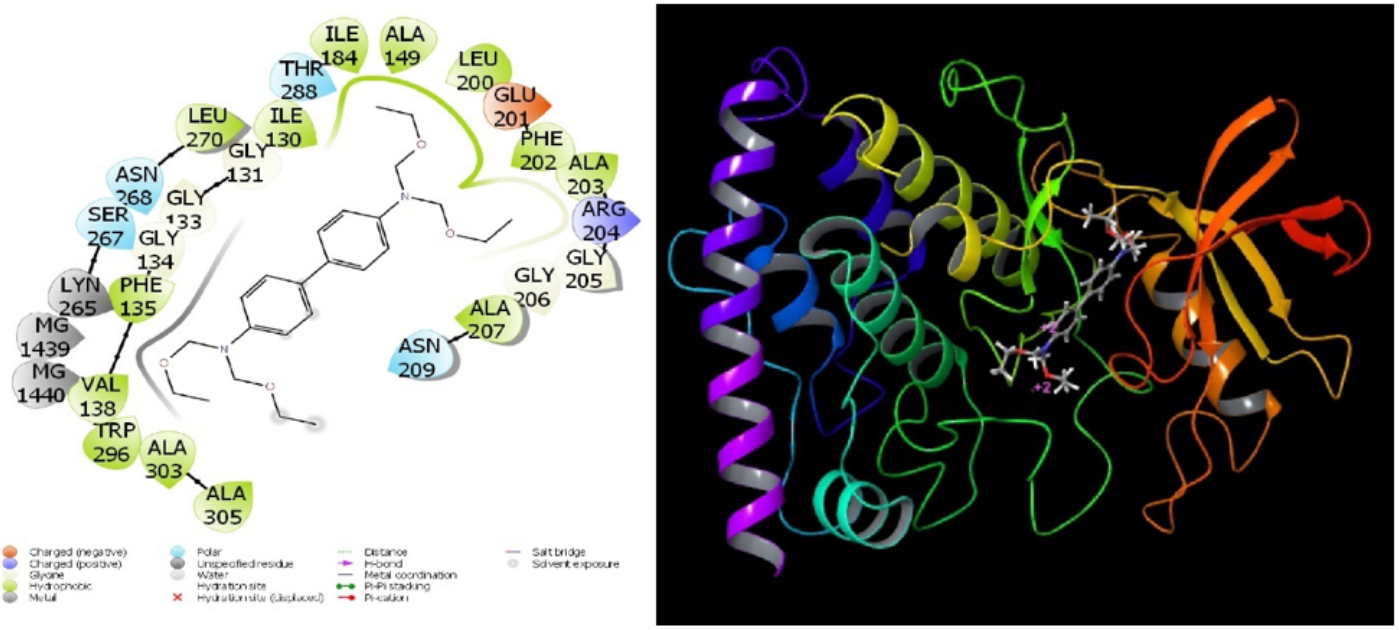

Figure 10

Presentation interactions of the compound 2 with colon cancer.

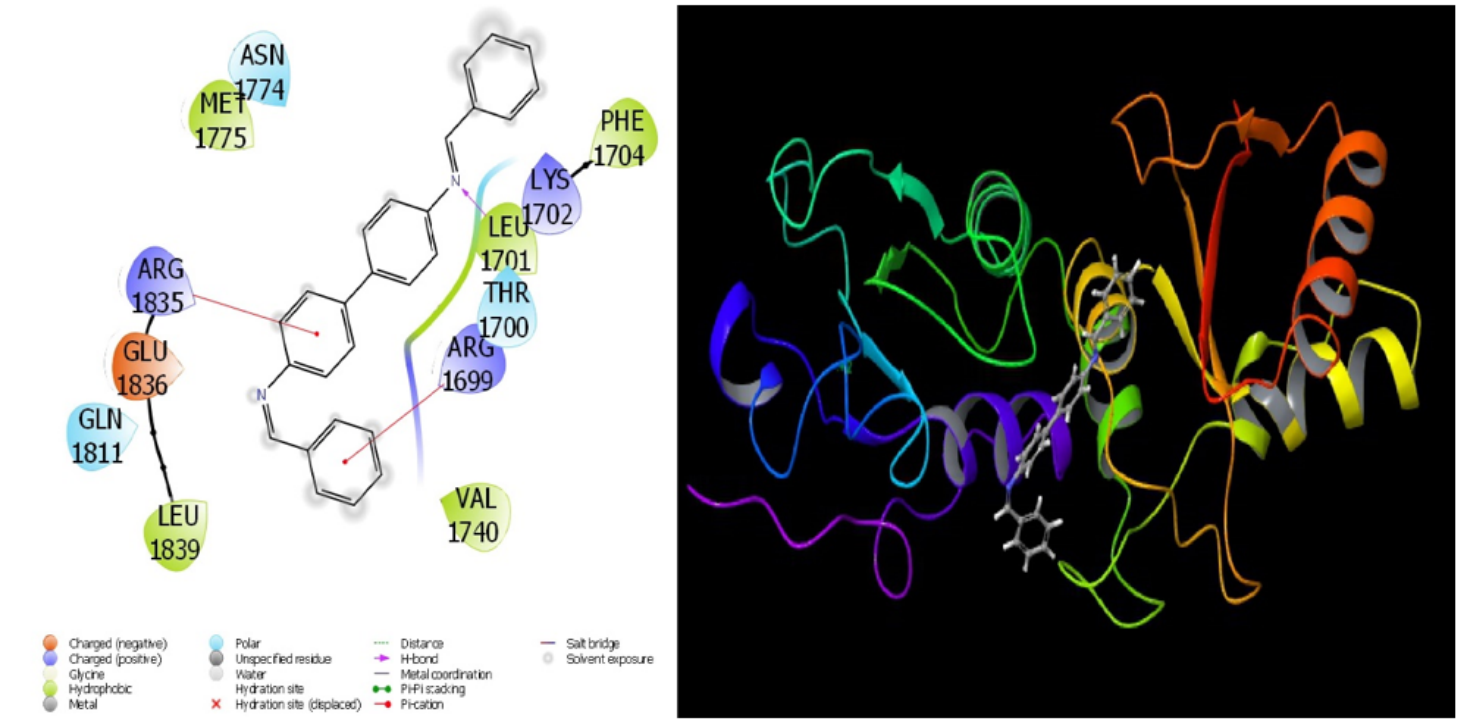

Figure 11

Presentation interactions of the compound 4a with breast cancer.

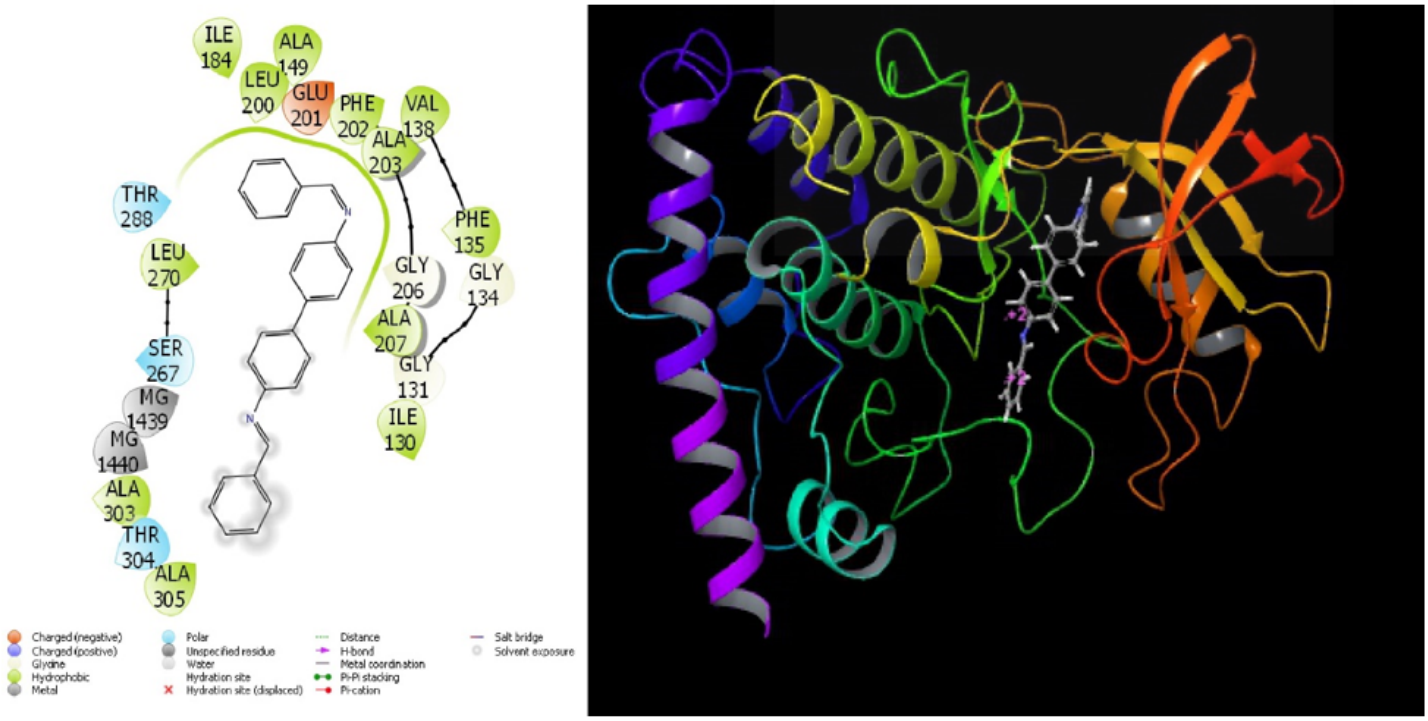

Figure 12

Presentation interactions of the compound 4a with colon cancer.

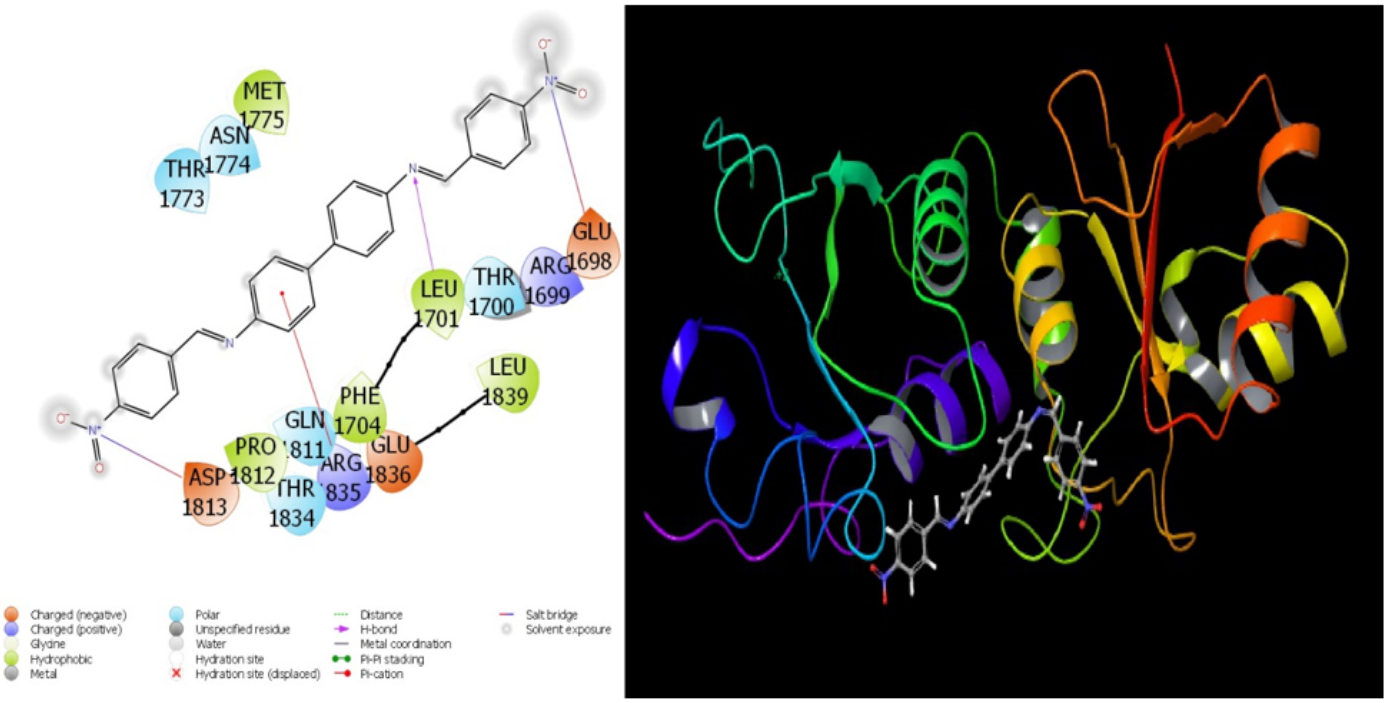

Figure 13

Presentation interactions of the compound 4b with breast cancer.

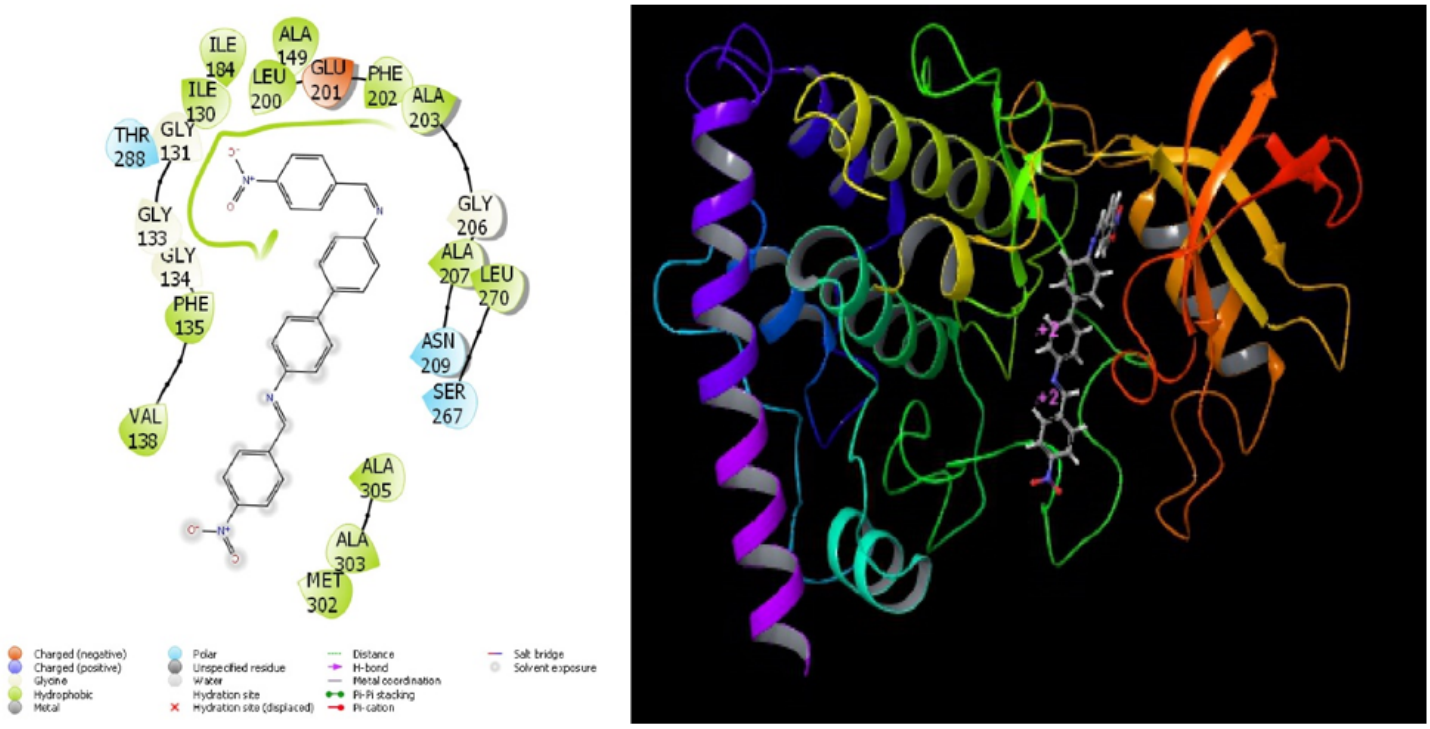

Figure 14

Presentation interactions of the compound 4b with colon cancer.

Supplementary Files

This is a list of supplementary files associated with this preprint. Click to download.

- GraphicalAbstract.docx
- schema1.png
- schema2.png